J|A|C|S COMMUNICATIONS

Published on Web 01/20/2010

A Strong Second-Harmonic Generation Material $Cd_4BiO(BO_3)_3$ Originating from 3-Chromophore Asymmetric Structures

Wei-Long Zhang, Wen-Dan Cheng,* Hao Zhang, Lei Geng, Chen-Sheng Lin, and Zhang-Zhen He

State Key Laboratory of Structural Chemistry, Fujian Institute of Research on the Structure of Mater, the Chinese Academy of Sciences, Fuzhou, Fujian 350002, China

Received October 26, 2009; E-mail: cwd@fjirsm.ac.cn

It is a great challenge to design new crystal materials with a preset function by an inorganic crystal engineering method.[1] A general strategy is suggested to employ noncentrosymmetric (NCS) chromophore as building units in the syntheses of NLO materials.[2−4] The NCS chromophore can consist of borate π-orbital systems[5,6] or distorted polyhedra with a d^0 cation center resulting from a second-order Jahn−Teller (SOJT) effect,[7−9] polar displacement of a d^{10} cation center,[10] or distortion from stereochemically active lone pair (SCALP) effect of cation.[11−13] To date, 2-chromophore structures as building units, for example, the unit constructed by asymmetric chromophores with SOJT d^0 and SCALP cation centers or with SCALP and delocalizationπ-orbital of borates, have been reported in the nonlinear optical (NLO) crystal materials.[7,8,14] It is expected that the cooperation effect of 3-chromophore asymmetrical structures will lead to a strong NLO response for designing the synthesis of a new compound. Here, we will report the synthesis, crystal structure, and NLO property of $Cd_4BiO(BO_3)_3$ compound with 3-chromophore asymmetrical structures.

Single crystals of $Cd_4BiO(BO_3)_3$ were prepared by the high temperature solid state reaction in the $CdO-Bi_2O_3-B_2O_3$ ternary system, and the obtained crystals (shown in Figure S1 of Supporting Information) by this reaction method have better chemical and thermal stability to ensure the feasibility of the industrial applications. The powder samples were synthesized from the stoichiometric mixtures of Bi_2O_3, CdO, and H_3BO_3, and their purities were confirmed by XRD powder diffraction studies. The measured XRD powder pattern (seen Figure S2 in Supporting Information) matches the one simulated from single-crystal X-ray diffraction studies.[15] Crystallographic analysis revealed that the $Cd_4BiO(BO_3)_3$ crystal belongs to the space group *Cm*. Its structure exhibits a complicated three-dimensional (3D) network composed of BiO_6, CdO_n ($n = 6$, 7) distorted polyhedra, and π-delocalization BO_3 groups that are interconnected via corner or edge sharing as shown in Figure 1a, b. In a $Cd1O_6$ octahedron, the Cd1−O2, Cd1−O3 (2) distances of 2.278, 2.313, and 2.327 Å are all shorter than the corresponding distances Cd1−O6, Cd1−O4 (2) of 2.286, 2.329, and 2.337 Å, and the $(Cd1)^{2+}$ cation displacement is along the 3-fold rotational axis of the octahedron that passes through the triangle faces O3O2O3′ and O4O6O4′, as shown in Figure 1d. This displacement of the cation leads to the loss of a symmetrical center of $Cd1O_6$ polyhedra. The $Cd2O_7$ is a distorted pentagonal bipyramid with Cd2−O bond distances ranging from 2.263(14) to 2.832(2) Å, as plotted in Figure 1e. $Cd1O_6$ and $Cd2O_7$ polyhedra are interconnected via sharing edges into a 1D double chain along the *c* axis (Figure S3 in Supporting Information). The double chains are further interconnected via a sharing corner into a 3D framework with the eight-member and four-member tunnels. Then, the B1 and Bi atoms are located in eight-member tunnels, while the B2 atoms are located in four-member tunnels. The 6-coordination Bi^{2+} is localized within the distorted octahedron BiO_6 resulting from the repulsive interactions between the lone-pair electron of Bi^{2+} and electron pairs of Bi−O bonding. There is a larger Bi−O1 distance of 2.472 Å and a smaller O1−Bi−O1′ angle of 144.1° (perfect value 180°) due to the repulsive interaction in the BiO_6 octahedron, as shown in Figure 1c (structure details seen in CIF in Supporting Information).

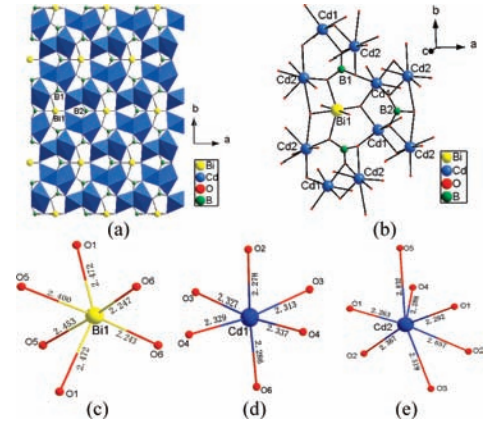

Figure 1. View of the structure of $Cd_4BiO(BO_3)_3$ down the *c* axis (a) and cation coordinate environments (b), and the coordination of oxygen atoms around Bi1 (c), Cd1 (d), and Cd2 (e) cations.

As mentioned above, the $Cd_4BiO(BO_3)_3$ is an NCS compound, and it prompts us to make NLO investigations. The SHG measurements on a Q-switched Nd:YAG laser with the sieved powder sample revealed that the SHG signal of $Cd_4BiO(BO_3)_3$ is ∼6.0 times that of a KDP standard of a similar grain size, shown in Figure 2a. Figure 2b shows a plot of second-harmonic intensity vs particle size of $Cd_4BiO(BO_3)_3$ powders. It finds that, for a particle size less than 100 μm, second-harmonic intensity linearly increases with increasing particle size and, for a particle size larger than 120 μm, second-harmonic intensity is essentially independent of particle size. This feature suggests that the compound is a phase-matchable material based on the SHG measurements of powder.[16] The SHG response of $Cd_4BiO(BO_3)_3$ is obviously larger than its isostructural compound $A_4M^{(III)}O(BO_3)_3$ (A = Ca; M = Nd, Gd, Sc, and Y).[17−19] The strong SHG response can be attributed to cooperation effects of the polarizations of the BiO_6 octahedra due to the Bi^{3+} cation SCALP, the asymmetric π-delocalization BO_3 groups, and the CdO_n polyhedra with a polar displacement of the d^{10} cation Cd^{2+}. Infrared (IR) spectroscopy measurement showed that $Cd_4BiO(BO_3)_3$ is IR transparent in the range 4000−1500 cm^{-1} (Figure S4a in Supporting Information), and the optical diffuse reflectance spectrum indicated an optical band gap of 3.16 eV and UV absorption cutoff edge at 392 nm as shown in Figure S4b of Supporting Information. The thermal analysis indicated that $Cd_4BiO(BO_3)_3$ is thermally stable up to ∼900 °C and melts congruently at 885 °C (Figure S5 in Supporting Information).

10.1021/ja9091209

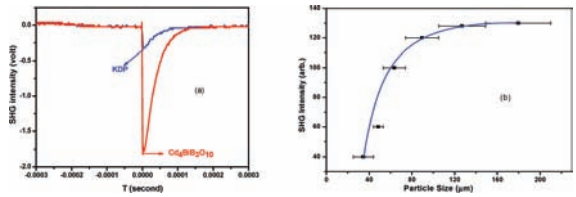

Figure 2. (a) Oscilloscope traces of the second harmonic generated signals KDP and $Cd_4BiO(BO_3)_3$. (b) Particle size vs SHG intensity of $Cd_4BiO(BO_3)_3$.

To gain insight into the relation between electronic structure and optical properties, we calculated the band structures and densities of states as well as electronic density differences by using the nonlocal gradient-corrected approximations of Perdew−Burke−Ernzerhof (PBE) functional and running code CASTEP for $Cd_4BiO(BO_3)_3$ (see section 2 of Supporting Information). The calculated band structures of Figure S6 (see Supporting Information) showed that $Cd_4BiO(BO_3)_3$ is an indirect gap material with a gap of 3.159 eV. The calculated total and partial densities of states (DOS) were plotted in Figure 3a. The band just above the Fermi level is predominately derived from Bi-6p, but with mixings of B-2p, and Cd-5s, and much less unoccupied O-2p states and least unoccupied Bi-6s states. However, the band just below the Fermi level is mostly composed of O-2p states and less mixed Bi-6s and Bi-6p states. The character shows that the SCALP effect of the Bi^{3+} cation results from the presence of mixings among the Bi-6s, -6p orbitals and ligand O-2p orbitals. To visualize this lone pair, we give the electron-density difference map containing the Bi−O1 plane in Figure 3b, where it well describes the polarization and charge transfer and clearly reveals highly asymmetric lobes on the Bi^{3+}cations. This asymmetric lobe may be thought of as SCALP. It is found from Figure 3a that the charge transfers across the band gap edge are contributions from the O-2p state to the B-2p and Bi-6p and Cd-5s states. That is, the charge transfers within the 3-chromophores including the BO_3, Bi-O_6, and CdO_n groups lead to a large SHG for the $Cd_4BiO(BO_3)_3$ compound. The evidence is also found in Figure 3b, for example, a decrease of O charges and an increase of cation charges in the B1−O1, Cd2−O4, Cd1−O2, and Bi−O1 linker zones (see also Figure S7 of Supporting Information).

The calculated six frequency-dependent SHG components of $Cd_4BiO(BO_3)_3$ were plotted in Figure S8 of the Supporting Information. The calculated largest and smallest tensor components, d_{11} and d_{33}, are 3.21 pm/V (7.67×10^{-9} esu) and 2.81 pm/V (6.70×10^{-9} esu) at a wavelength of 1064 nm (1.165 eV) for $Cd_4BiO(BO_3)_3$, respectively. These values are close to our experimental value, which is 6 times that of KDP ($d_{36} = 1.1 \times 10^{-9}$ esu), and they are larger than the d_{ij} values of BiB_3O_6 (the largest and smallest values of expt $d_{16} = 2.8$, $d_{23} = 0.9$ pm/V; calcd $d_{22} = 2.95$, $d_{23} = 1.17$ pm/V).[20] Comparing the structures and compositions of $Cd_4BiO(BO_3)_3$ and $BiBO_3O_6$, we find that larger NLO coefficients of $Cd_4BiO(BO_3)_3$ that arise may be from the CdO_n group with a polar displacement of the d^{10} cation Cd^{2+}. In fact, it is the largest NLO coefficient for $Cd_4BiO(BO_3)_3$ among borate systems.[5,20]

In summary, we have designed a novel SHG crystal material $Cd_4BiO(BO_3)_3$ with the largest NLO coefficient among borates. The strong SHG effect originates from the cooperation of the 3-chromophore asymmetric structures composed of the polar displacement

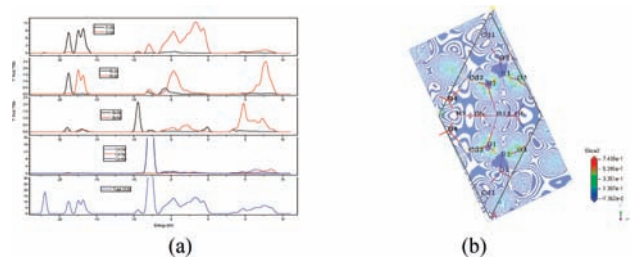

Figure 3. (a) Density of states and partial density of states and (b) the plot of electronic density difference for $Cd_4BiO(BO_3)_3$.

of the d^{10} Cd^{2+} ion, SCALP effect of Bi^{3+}, and π-delocalization of BO_3. The features of phase match, high thermal stability, and congruent melting are favorable in industrial production and applications for crystal $Cd_4BiO(BO_3)_3$. In the future, we will continue to explore the compounds of the $A_4BiO(BO_3)_3$ system (A = Ca^{2+}, Ba^{2+}, and Pb^{2+}) and their optical properties.

Acknowledgment. This investigation was based on work supported by the National Natural Science Foundation of China under Project 20773131, the National Basic Research Program of China (No. 2007CB815307).

Supporting Information Available: Details of crystallographic studies, physical property measurements, and theoretical calculations for $Cd_4BiO(BO_3)_3$. This material is available free of charge via the Internet at http://pubs.acs.org.

References

(1) Brammer, L. *Chem. Soc. Rev.* **2004**, *33*, 476–489.
(2) Evans, O. R.; Lin, W. *Chem. Mater.* **2001**, *13*, 2705–2712.
(3) Bells, S. D.; Ratner, M. A.; Marks, T. J. *J. Am. Chem. Soc.* **1992**, *114*, 5842–5849.
(4) Bera, T. K.; Jang, J. I.; Ketterson, J. B.; Kanatzidis, M. G. *J. Am. Chem. Soc.,* **2009**, *131*, 75–77.
(5) Sasaki, T.; Mori, Y.; Yoshimura, M.; Yap, Y. K.; Kamimura, T. *Mater. Sci. Eng., R* **2000**, *30*, 1–54.
(6) Pan, S.; Smit, J. P.; Watkins, B.; Marvel, M. R.; Stern, C. L.; Poeppelmeier, K. R. *J. Am. Chem. Soc.* **2006**, *128*, 11631–11634.
(7) Ra, H. S.; Ok, K. M.; Halasyamani, P. S. *J. Am. Chem. Soc.* **2003**, *125*, 7764–7765.
(8) Sykora, R. E.; Ok, K. M.; Halasyamani, P. S.; Albrecht-Schmitt, T. E. *J. Am. Chem. Soc.* **2002**, *124*, 1951–1957.
(9) (a) Chi, E. O.; Ok, K. M.; Porter, Y.; Halasyamani, P. S. *Chem. Mater.* **2006**, *18*, 2070–2074. (b) Phanon, D.; Gautier-Luneau, I. *Angew. Chem., Int. Ed.* **2007**, *46*, 8488–8491.
(10) Inaguma, Y.; Yoshida, M.; Katsumata, T. *J. Am. Chem. Soc.* **2008**, *130*, 6704–6705.
(11) Kim, S.-H.; Yeon, J.; Halasyamani, P. S. *Chem. Mater.* **2009**, *21*, 5335–5342.
(12) Phanon, D.; Gautier-Luneau, I. *Angew. Chem., Int. Ed.* **2007**, *46*, 8488–8491.
(13) Chang, H.-Y.; Kim, S.-H.; Ok, K. M.; Halasyamani, P. S. *J. Am. Chem. Soc.* **2009**, *131*, 6865–6873.
(14) Kong, F.; Huang, S.-P.; Sun, Z.-M.; Mao, J.-G.; Cheng, W.-D. *J. Am. Chem. Soc.* **2006**, *128*, 7750–7751.
(15) Crystal data for $Cd_4BiO(BO_3)_3$: $M_r = 851.05$, monoclinic *Cm* with $a = 8.044(2)$ Å, $b = 15.913(5)$ Å, $c = 3.4891(10)$ Å, $\beta = 100.08(2)°$, $V = 439.7(2)$ Å^3, $Z = 2$. The final least-squares refinements converged at R1 (wR2) = 0.0383 (0.0806) and $S = 1.042$ for 989 reflections with $I > 2\sigma(I)$.
(16) Kurtz, S. K.; Perry, T. T. *J. Appl. Phys.* **1968**, *39*, 3798–3813.
(17) Aka, G.; Mougel, F.; Augé, F.; Kahn-Harari, A.; Vivien, D.; Bénitez, J. M.; Salin, F.; Pelenc, D.; Balembois, F.; Georges, P.; Brun, A.; Le Nain, N.; Jacquet, M. *J. Alloys Compd.* **2000**, *401*, 303–304.
(18) Gheorghe, L.; Loiseau, P.; Aka, G.; Lupei, V. *J. Cryst. Growth* **2006**, *294*, 442–446.
(19) Aka, G.; Brenier, A. *Opt. Mater.* **2003**, *22*, 89–94.
(20) Lin, Z. S.; Wang, Z. Z.; Chen, C. T.; Lee, M. H. *J. Appl. Phys.* **2001**, *90*, 5585–5590.

(W.-D. Cheng)

JA9091209